Observation-constrained multicycle dynamic models of southern San Andreas fault and the San Jacinto fault: effects of the Cajon Pass and the Big Bend on rupture dynamics

Dunyu Liu and Benchun Duan

09/04/2020

SCEC Cajon Pass Earthquake Gate Area: Progress and Future Plans

Department of
GEOLOGY & GEOPHYSICS
COLLEGE OF GEOSCIENCES
TEXAS A&M HIGH PERFORMANCE RESEARCH COMPUTING

SCEC
AN NSF+USGS CENTER

Outline

- Why do we need multicycle dynamic models?
- Fault geometry, method, loading, and constraints from observations.
- Results from numerical models.
- Comparisons between models and observations.
- Summary

Why do we need multicycle dynamic models?

- ❑ Uncertainties: stress, geometry, friction, rheology, thermal process…
- ❑ A multidisciplinary approach: linking observations from different fields.
- ❑ Keys: geometry, earthquake cycles, dynamic rupture

- Why fault geometric complexities?
  - Prevalence in nature (e.g., *Wesnousky*, 2006).
  - Conditional barriers to ruptures → Earthquake gates (*Oskin et al.*, 2015; *Biasi and Wesnousky*, 2017; *Duan et al.*, 2019;).
  - Rupture extents

- Why earthquake cycles?
  - Uncertainties in initial stress condition before an earthquake.
  - Reproduce past earthquake pattern or statistics.

- Why dynamic ruptures?
  - Typically ignored in long-term earthquake cycles.
  - However, they induce large stress perturbations. (e.g., *Harris and Day*, 1993; *Kame et al.*, 2003; *Dunham et al.*, 2011b; *Lozos et al.*, 2011; *Ryan and Oglesby*, 2014; *Luo and Duan*, 2018)

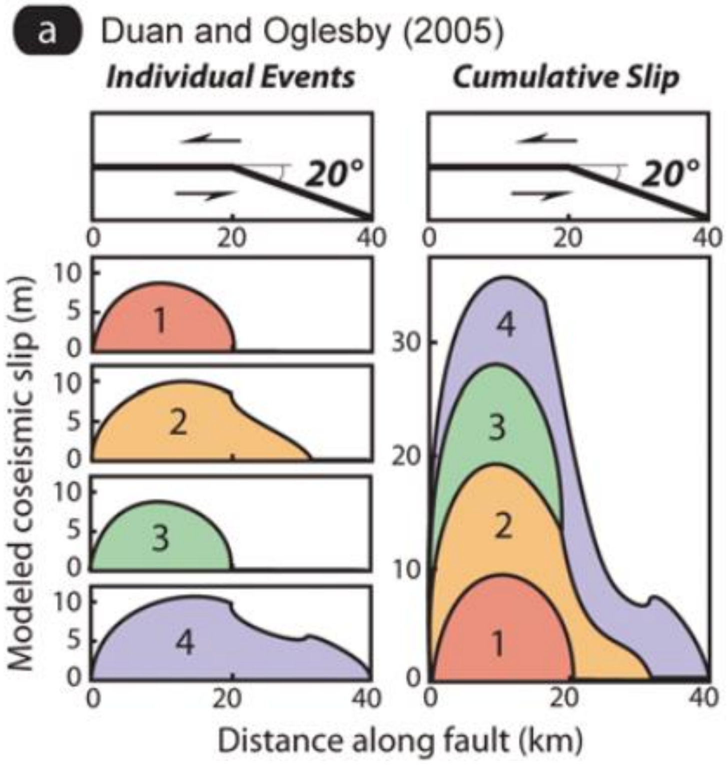

A feedback loop

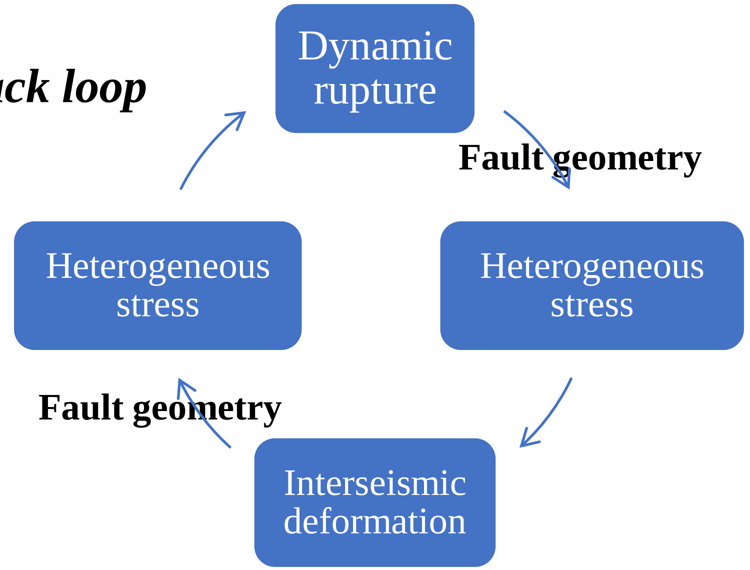

(Liu, Duan, Prush, Oskin and Liu-Zeng, in preparation)

- What is the potential rupture extent of the next big earthquake in southern California and when? If we could reproduce what happened in the past, we might be able to have a clue for what would happen in the future.

- Because of the rupture extent of the 1857 Fort Tejon earthquake, the Cajon Pass earthquake gate and the Big Bend, where fault strike changes dramatically over a wide range, should be considered in one model.

Fault geometry

- CFM 5.2 (*Nicholson et al.*, 2017; *Plesch et al.*, 2007), 3 km depth.
- SAF: Carrizo + Big Bend + Mojave + San Bernardino
- SJF: Claremont + Clark

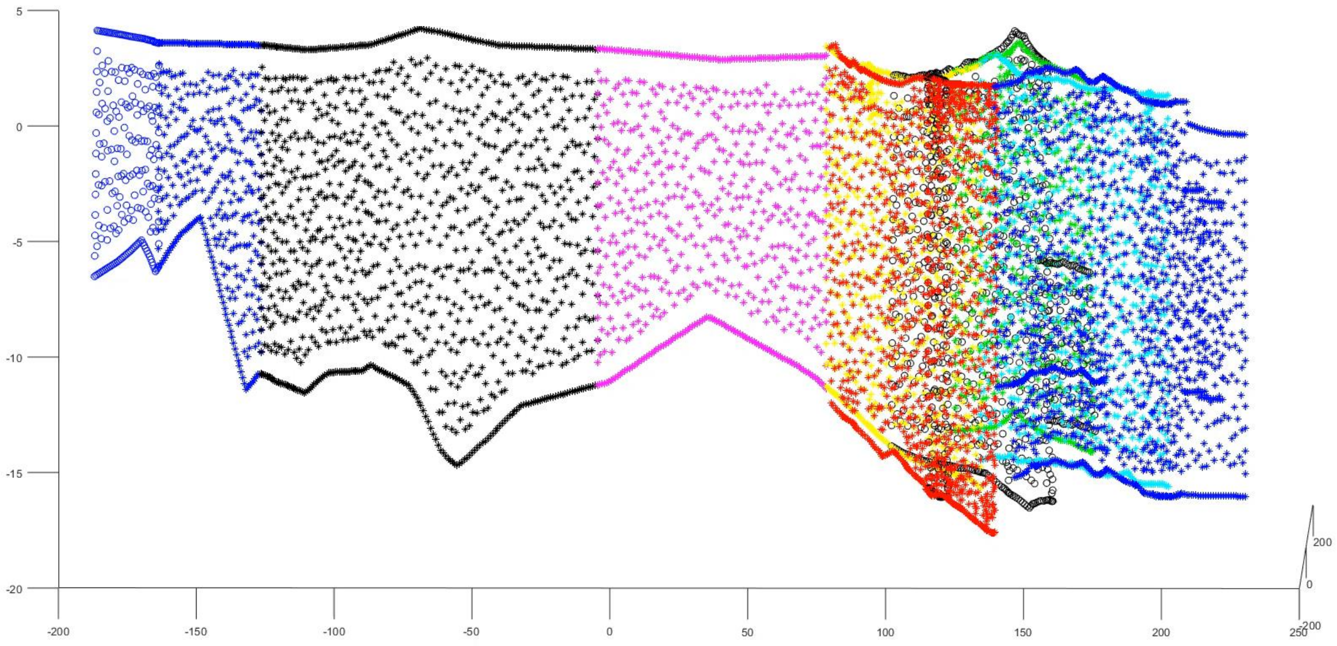

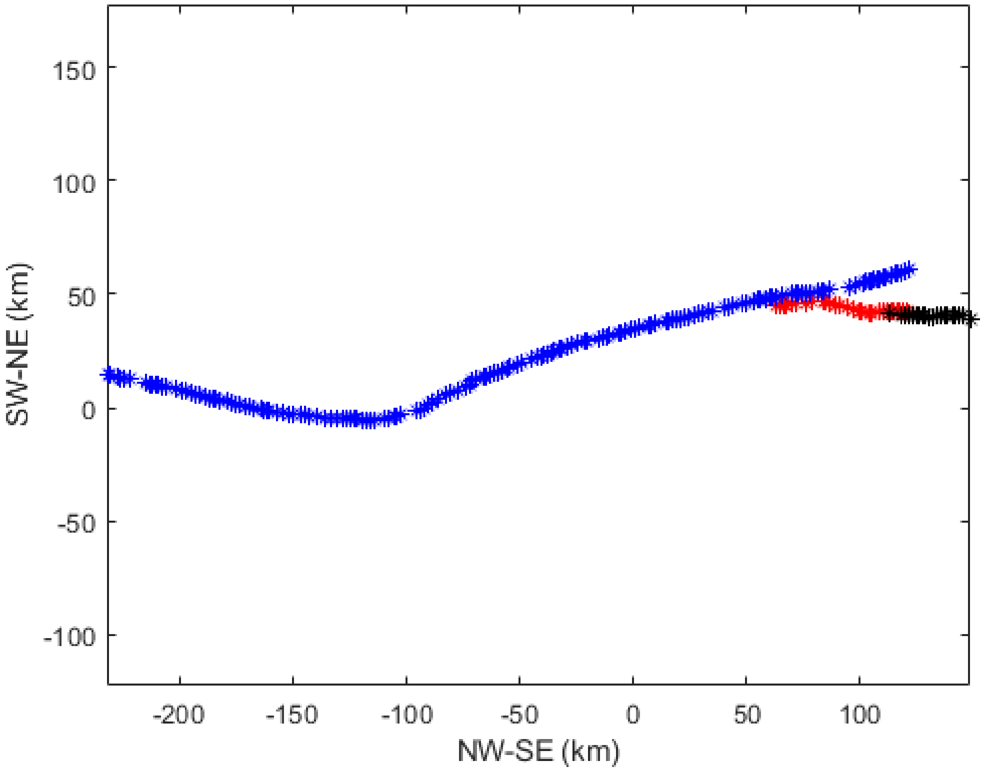

2D finite element method for multicycle dynamics on geometrically complex fault systems

- The FEM consists of EQdyna 2D (e.g., *Duan and Oglesby*, 2006) , a finite element code for co-seismic dynamic ruptures and viscoelastic solution for stress relaxation and interseismic stress evolution.
  - Assuming the region is under pure shearing and the maximum shear strain rate is γ, the normal γ_n and shear loading rate γ_τ are calculated by eq (1) and (2). Normal and shear stresses evolve based on eq (3) and (4).
  - $\gamma_n = \gamma \sin(2\phi)$ (1),
  - $\gamma_\tau = \gamma \cos(2\phi)$ (2),
  - $\sigma_\tau(t) = \left(\sigma_\tau^{last} - \eta\gamma_\tau\right) \exp\left(-\frac{\mu}{\eta} t\right) + \eta\gamma_\tau$ (3),
  - $\sigma_n(t) = \left(\sigma_n^{last} - \sigma_n^{backg} - \eta\gamma_n\right) \exp\left(-\frac{\mu}{\eta} t\right) + \eta\gamma_n + \sigma_n^{backg}$ (4).
  - μ is shear modulus, η is viscosity, σ_n^{backg} is the ambient stress, ϕ is the angle difference between the fault local strike and the maximum shear direction.
- *Duan* (2019) and *Duan et al.* (2019) apply the method to the Aksay bend earthquake gate of the Altyn Tagh fault in northwest China. Realistic fault geometry is used.

2D finite element method, Cont.

- The friction law used in dynamic ruptures is the slip- and rate- weakening law (*Duan*, 2019) in the following form
- $f_1(d) = \begin{cases} f_s - \frac{(f_s - f_d)d}{d_0}, d \le d_0 \\ f_d, \quad d > d_0 \end{cases}$
- $f_2(v) = \begin{cases} f_r - \frac{(f_r - f_d)v}{v_0}, v \le v_0 \\ f_d, \quad v > v_0 \end{cases}$
- $f(d, v) = \max(f_1(d), f_2(v))$

- f_s, f_d, f_r are static, dynamic and restrengthening friction coefficient, respectively. d_0, v_0 are critical slip distance and critical slip velocity in the slip- and rate- weakening law.

Straining rate and direction

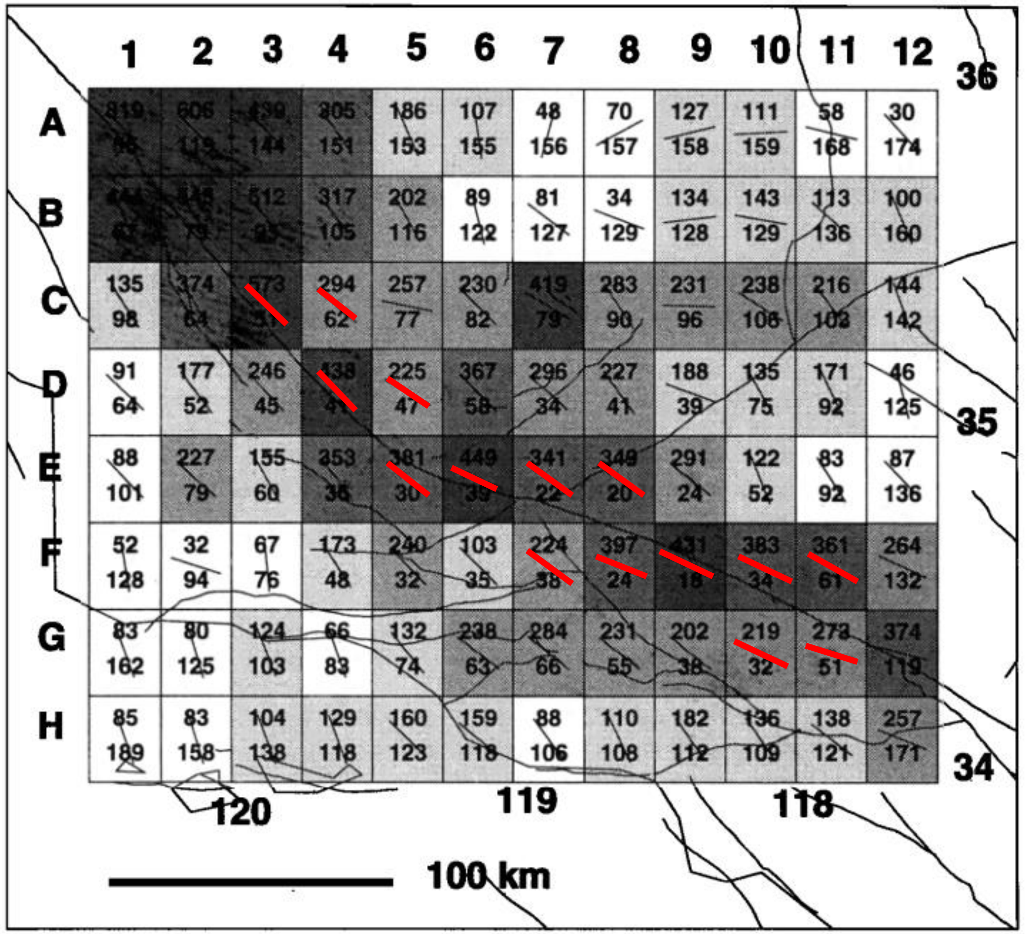

(*Snay et al.*, 1996)

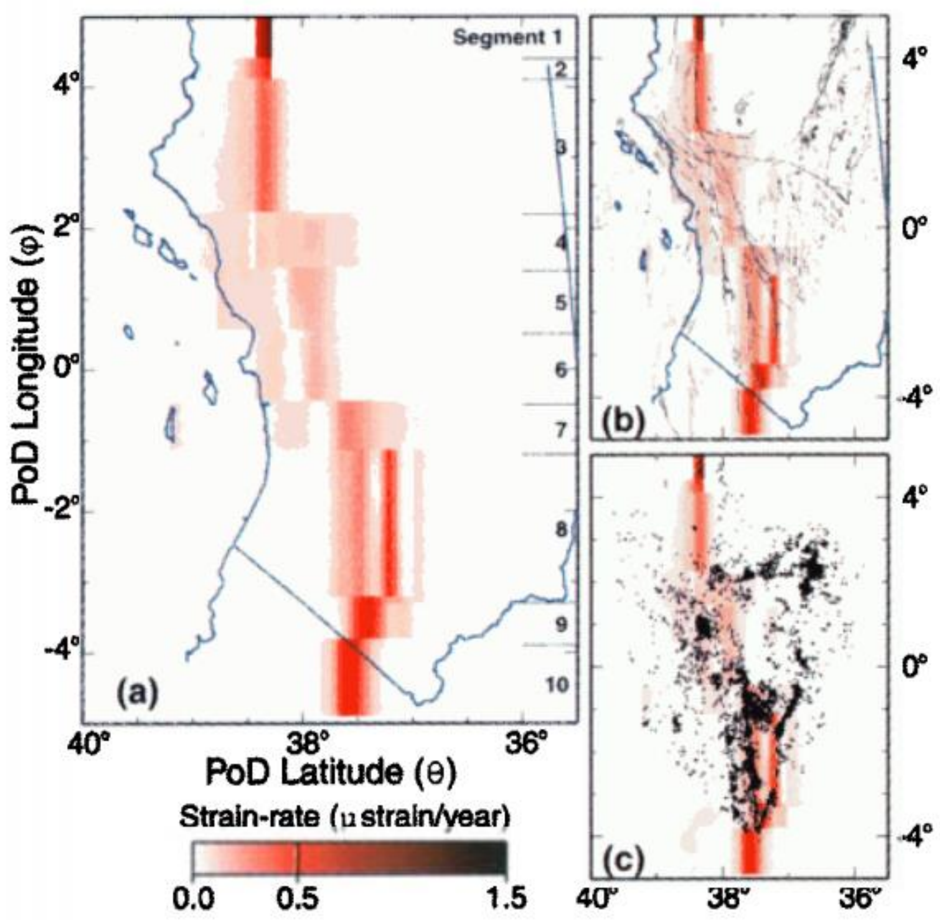

(*Wdowinski et al.*, 2001)

Model input

- Loading rate:
  - *Snay et al.* (1996)
  - *Wdowinski et al.* (2001)

- Loading direction:
  - *Snay et al.* (1996)
  - *Gilbert et al.* (1994)
- Model A
  - Preferred
  - Loading rate: Wdowinski01
  - Loading direction:
    - Parallel+Compressional
- Model B
  - End member
  - Loading rate: Snay96
  - Loading direction: Gilbert94
- Model C
  - End member
  - Uniform loading

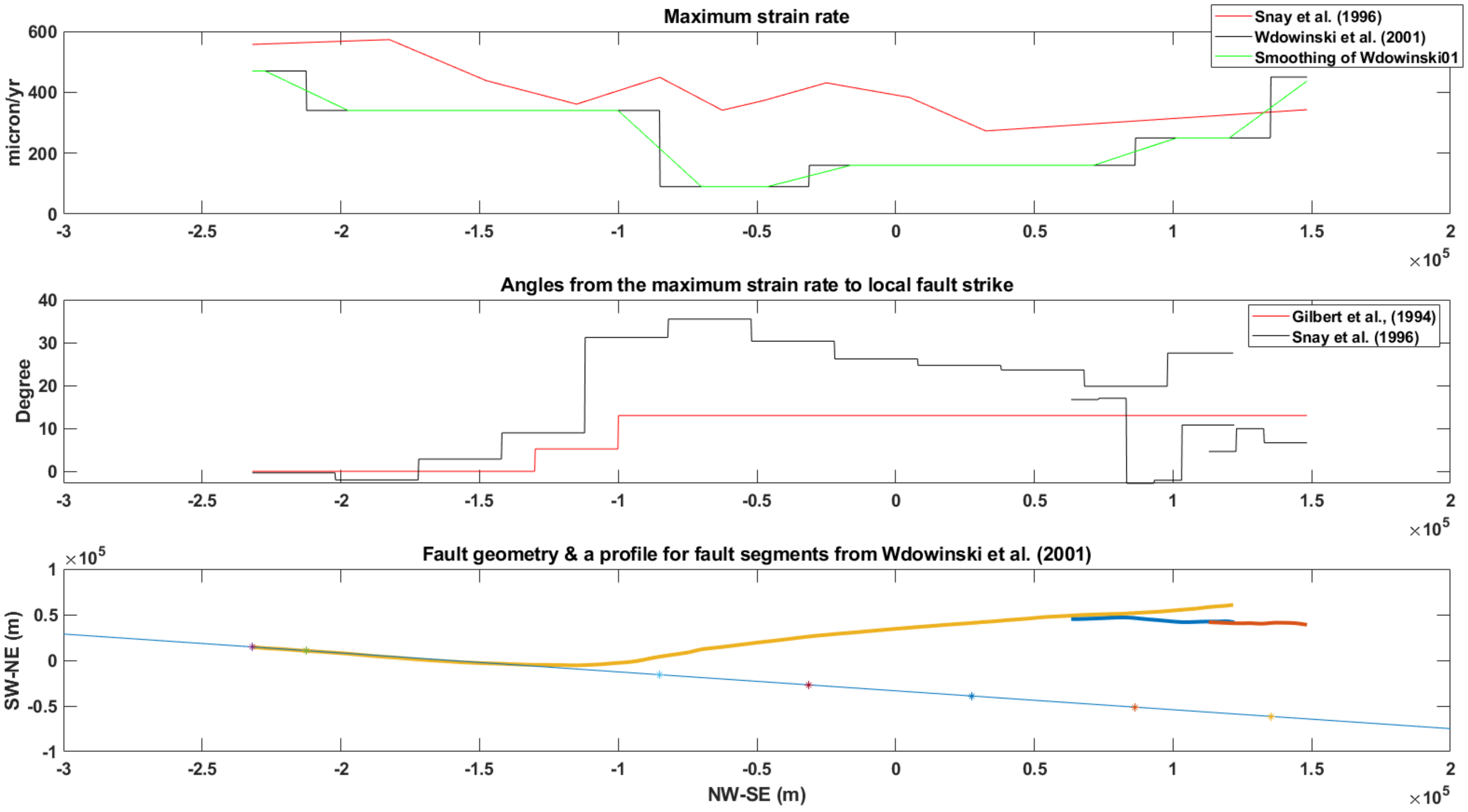

Constraints

- Long-term slip rate
  - SAF: about 13-34 mm/yr
  - SJF: about 2.5-12 mm/yr

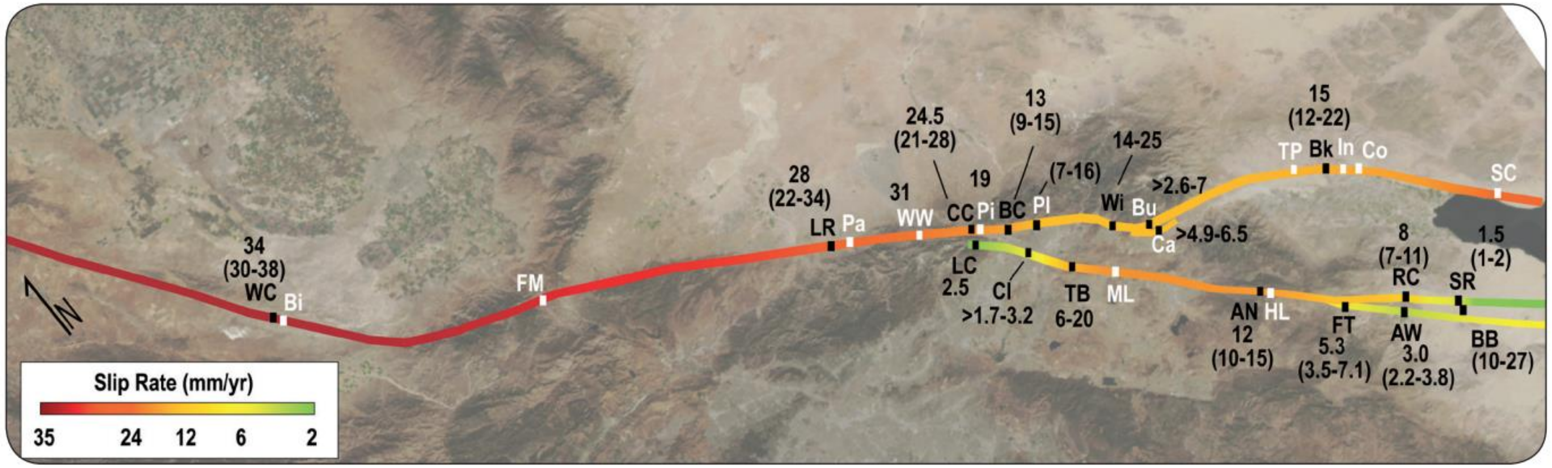

Rockwell et al. (2016)

- Slip per event
  - ~5 m at Carrizo plain (*Zielke et al.*, 2010)

Rupture dynamics of Model A

- Maximum shearing direction
  - Parallel
  - 10° compressional
  - Rate (Wdowinski)
- $\sigma_n^{backg} = -100$ MPa
- f_s, f_d, f_r: 0.4, 0.365, 0.39

- Dynamic ruptures
  - A: breaking the whole system;
  - B: breaking SAF north of the Big Bend;
  - C: breaking parts of individual SJF, SAF segments.

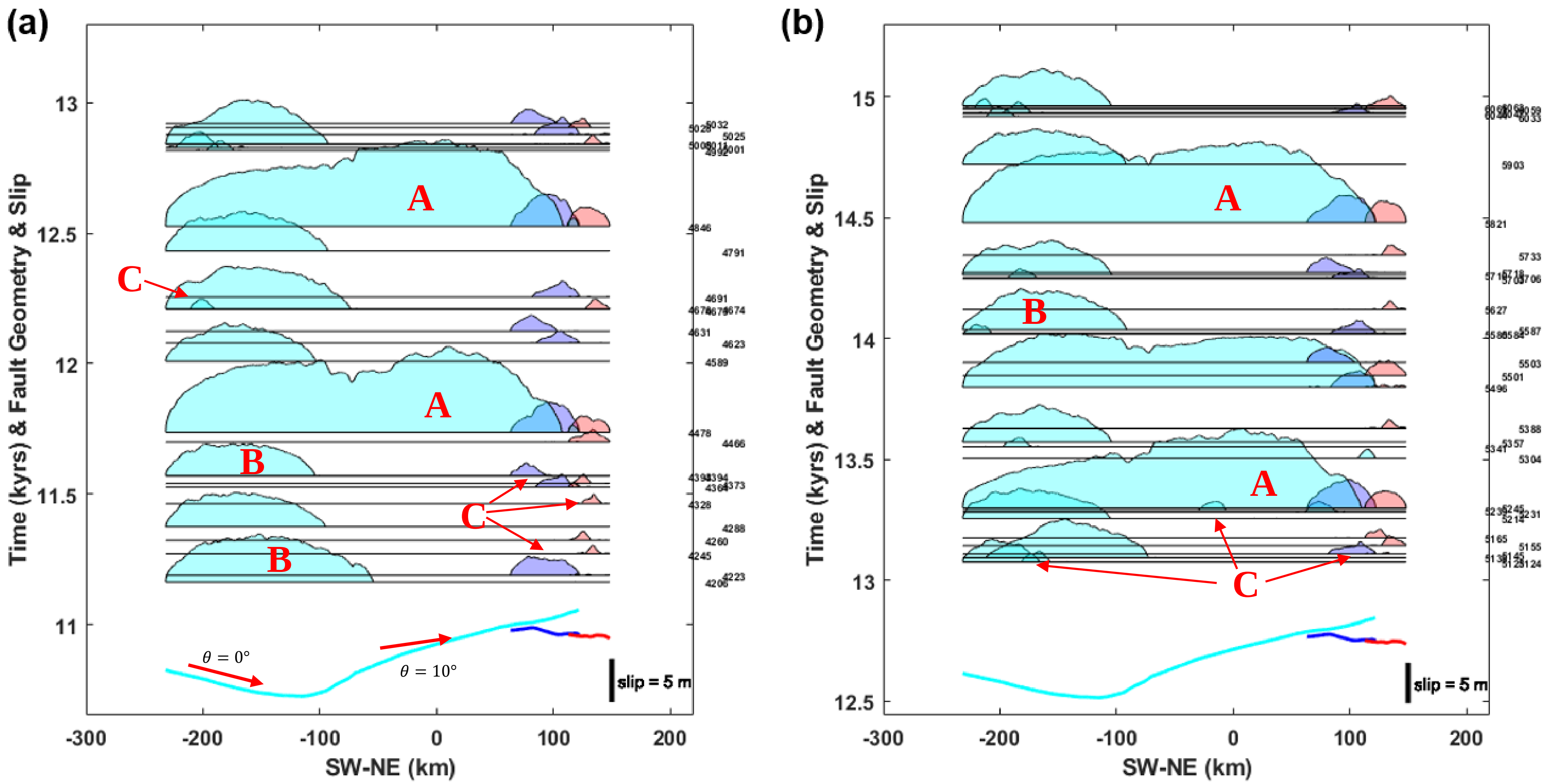

Earthquake sequence of Model A

Heterogeneous stress

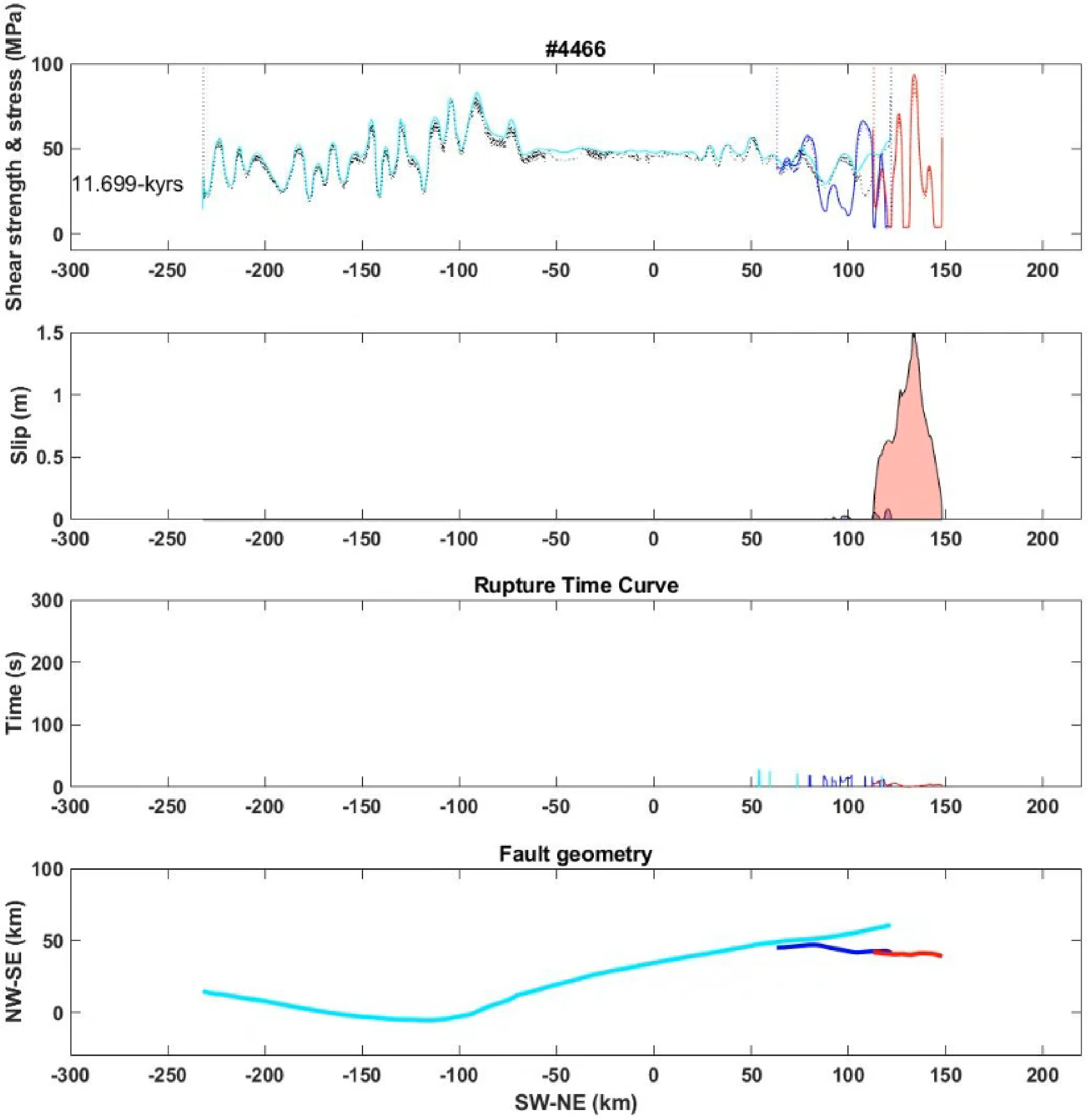

Possible epicenters

Large ruptures could start near Cajon Pass or north of the Big Bend, presenting different seismic shaking hazard.

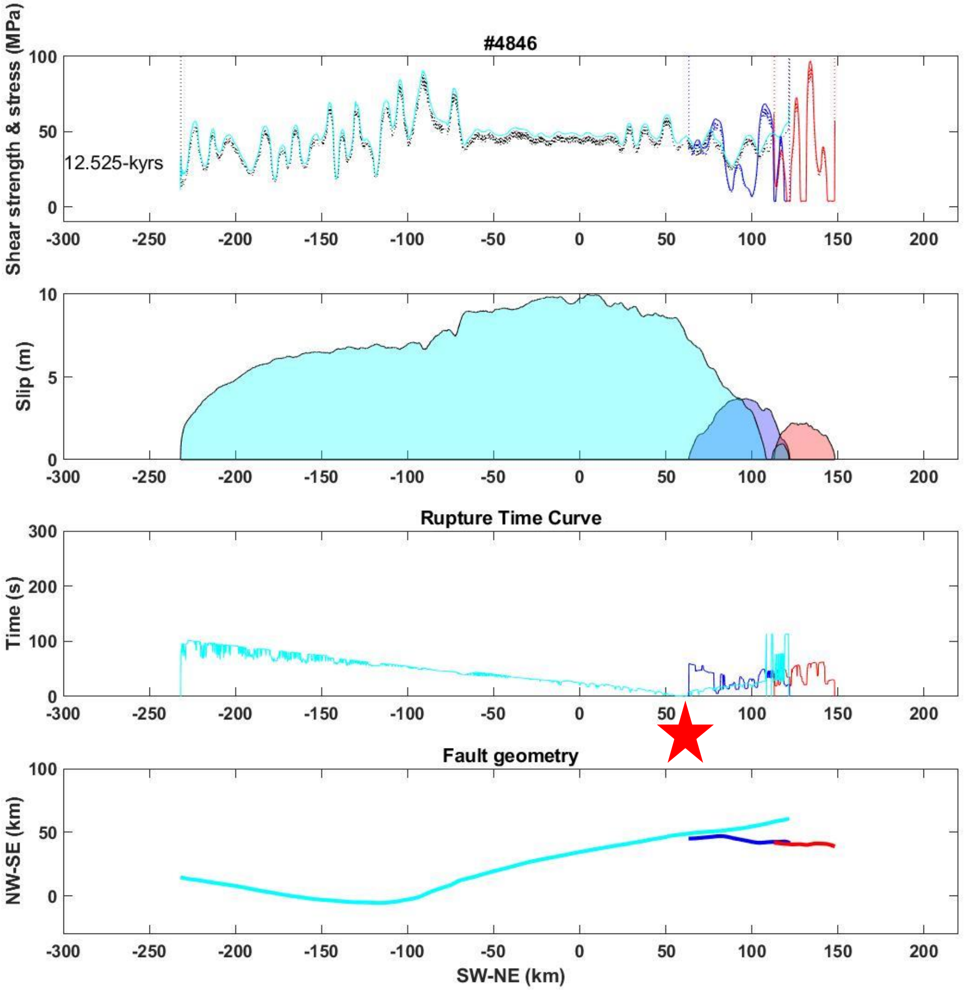

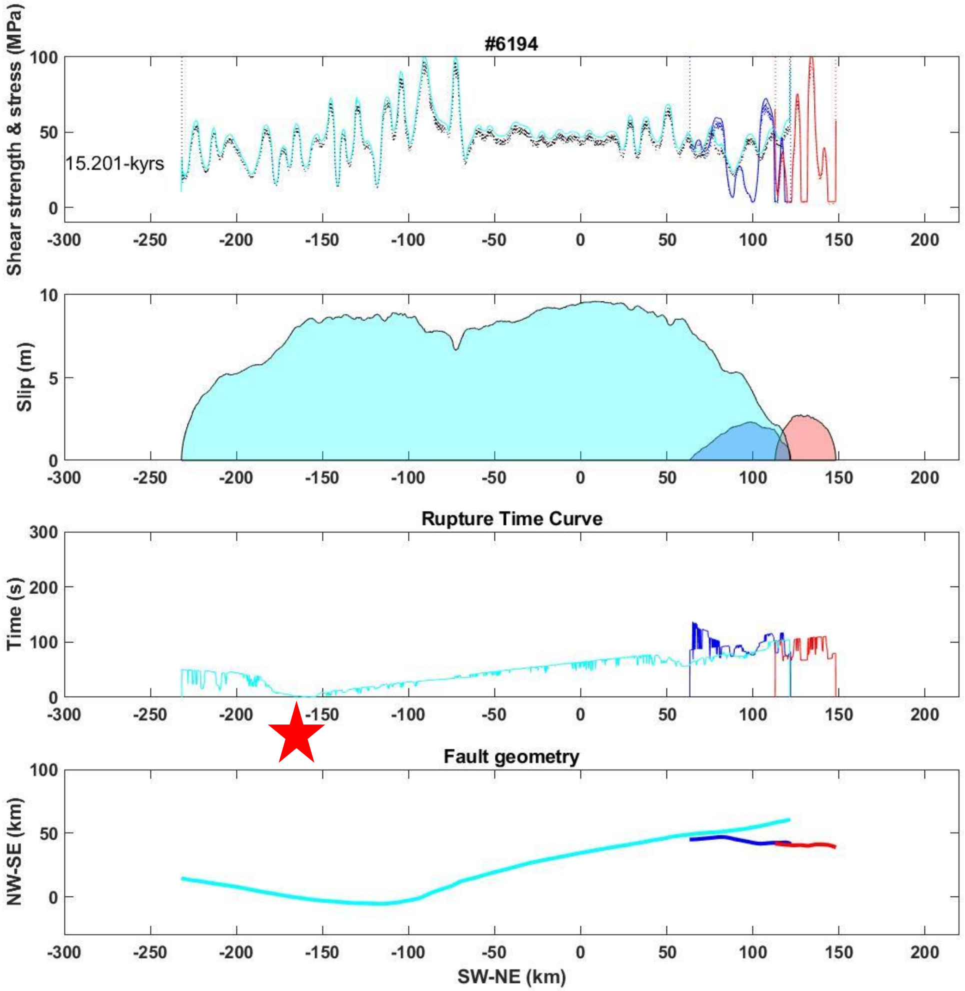

Rupture dynamics of Model B

- Maximum shearing direction
  - Parallel (*Gilbert et al.*, 1994)

- Dynamic ruptures
  - A: breaking the whole system;
  - C: breaking parts of individual SJF, SAF segments.

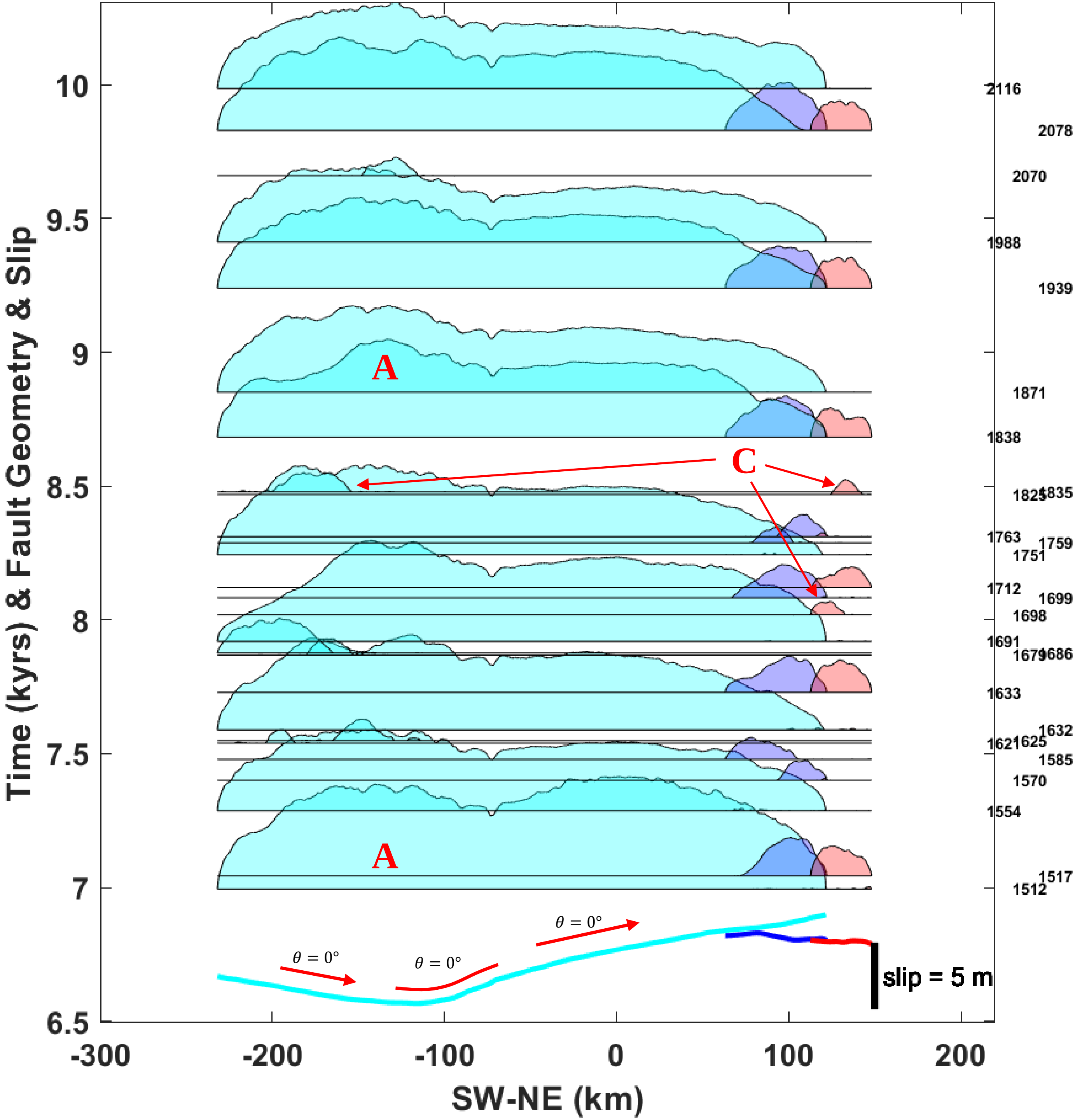

Rupture dynamics of Model C, uniform loading

- With uniform loading in terms of both rate and direction, the big bend is a stronger barrier to ruptures.

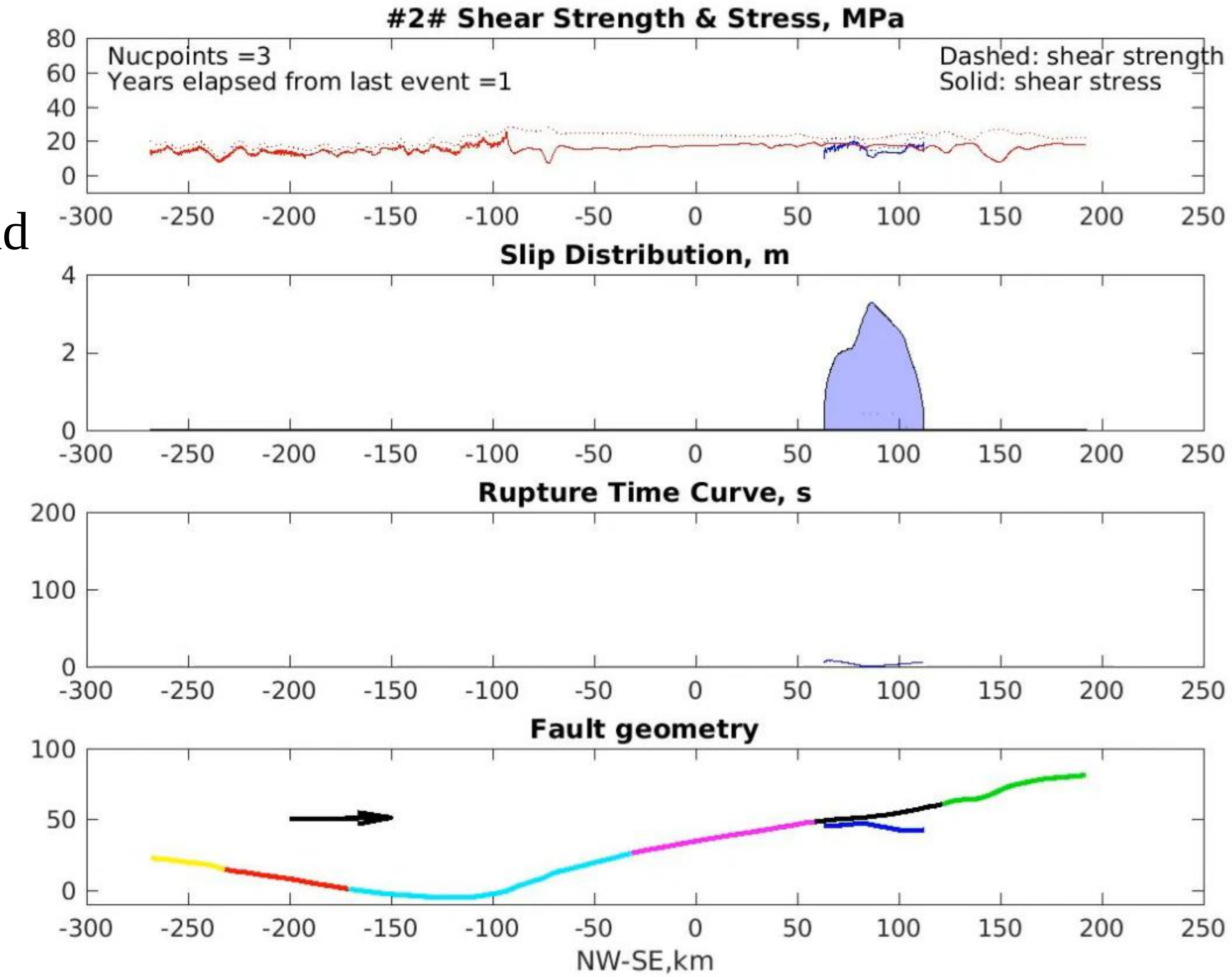

Long term slip rates

- Model A:
  - Parallel + compressional
  - Wdowinski01 rate.
- Model B:
  - parallel (Gilbert94)
  - Snay96 rate (generally higher than Wdowinski01 rate, especially south of the Big Bend).
- Model D: fs=0.5
- Model E: like Model B but with higher viscosity.

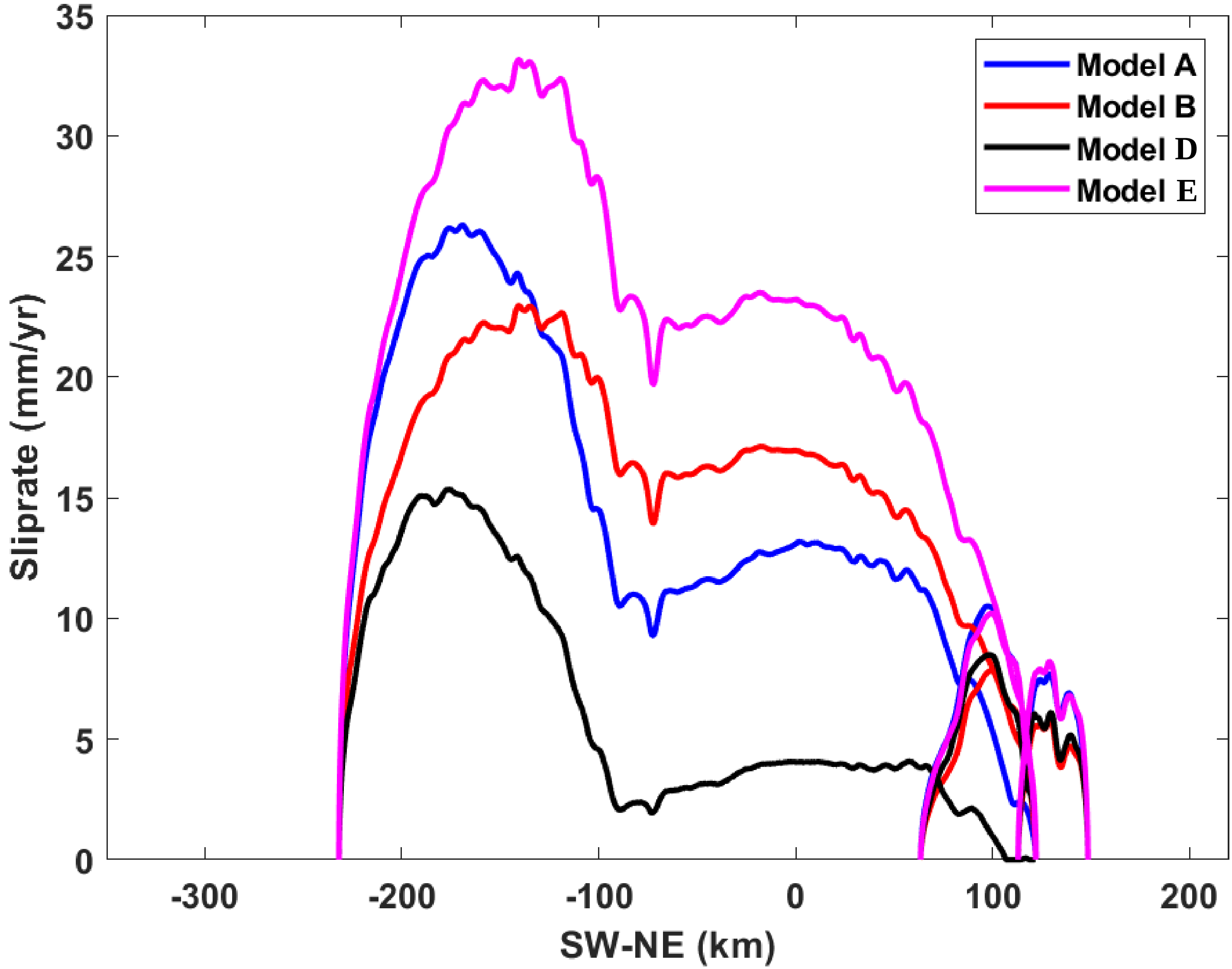

Comparisons to rupture extents from paleoseismicity

- Models could reproduce events 13, 17, 20, 23, 35, 41 on SAF and 2, 4, 7, 8, 12, 21, 25, 42, 45, 48, 50 on SJF.
- Events like 11, 26 on SAF are shown in some models.
- Potential 17-like rupture for 33, 37, 43-46 based on numerical results?
- Based on numerical results, potential combined rupture of both SAF and SJF?
- A more quantitative comparison between numerical models and paleoseismological records in terms of both rupture extents and recurrence intervals?

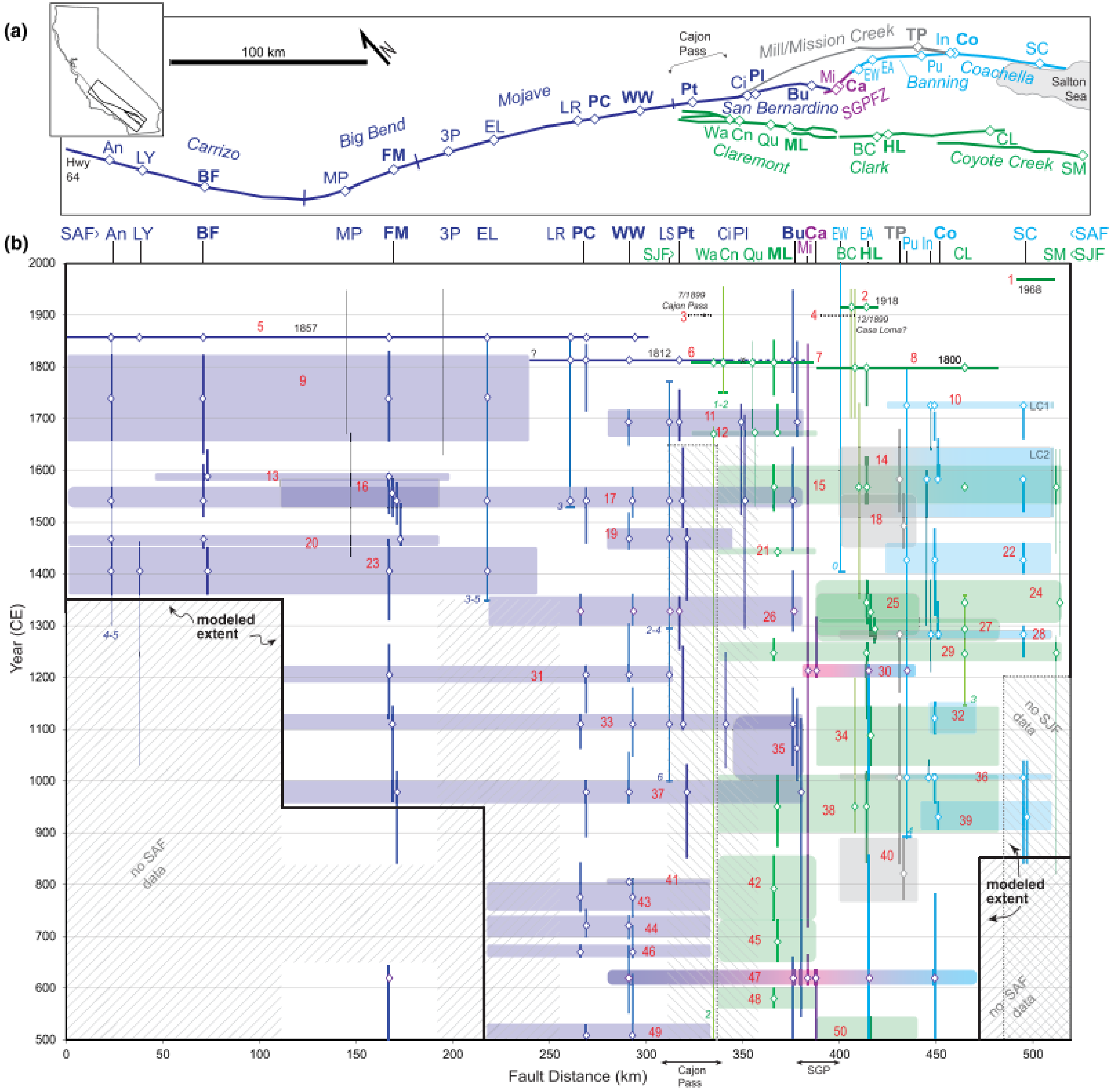

(*Scharer and Yule*, 2020)

Summary

- 2D multicycle dynamic models of the southern SAF and SJF are simulated. Realistic fault geometry is used. The loading comes from geodetic observations and results are compared to long-term slip rate, slip-per-event estimation, rupture extents inferred from paleoseismological records.
- Results indicate that the southern San Andreas fault and the San Jacinto fault could break in one event with epicenters either near Cajon Pass or north of the Big Bend.
- Fault geometry control rupture extents for some events such as those terminated by the Big Bend, and ruptures breaking parts of SAF and SJF fault segments.
- Complex rupture extents inferred from paleoseismological records could be largely reproduced by the multicycle dynamic models. It indicates the key roles of dynamic rupture and fault geometry over earthquake cycles.

Thank you!

Acknowledgement

- The studies were/are funded by SCEC Award 19238 and 20138.
- We appreciate Texas A&M High Performance Research Computing (http://hprc.tamu.edu/) for providing the advanced computing resources used in the study.

1812-like ruptures

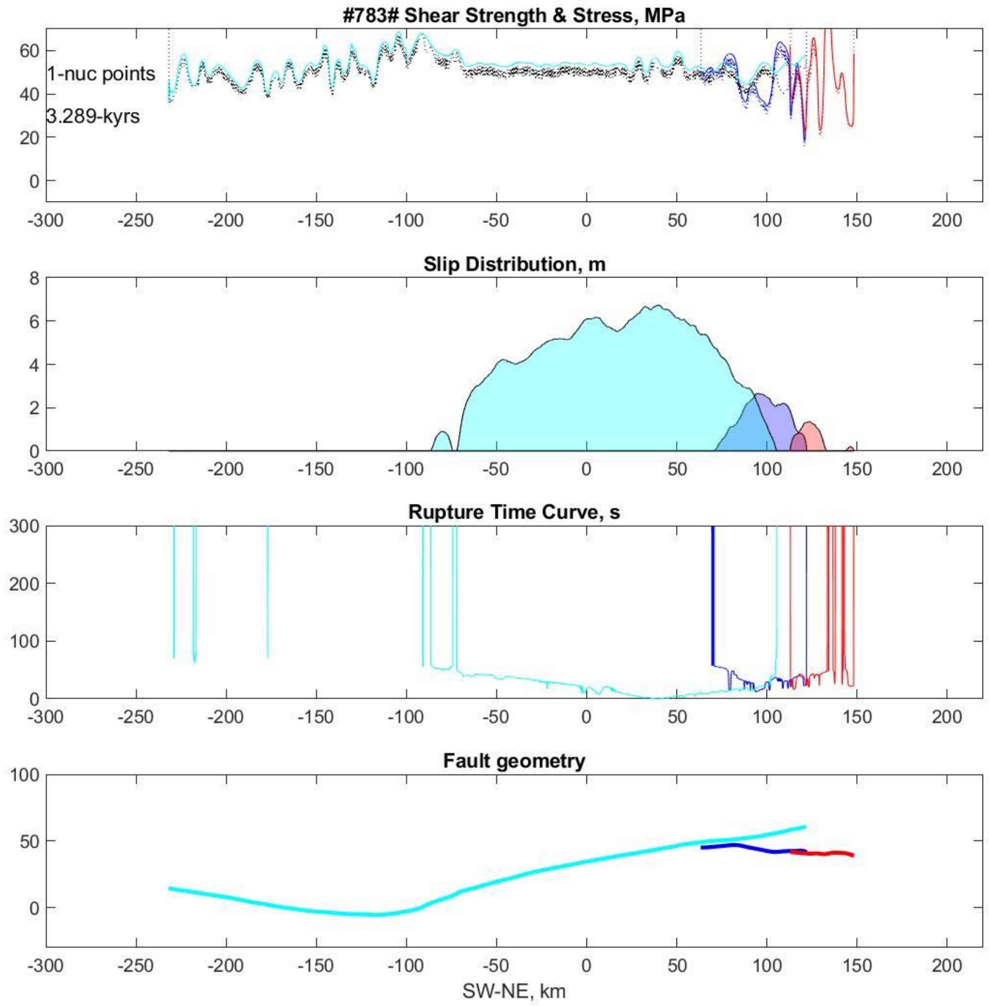

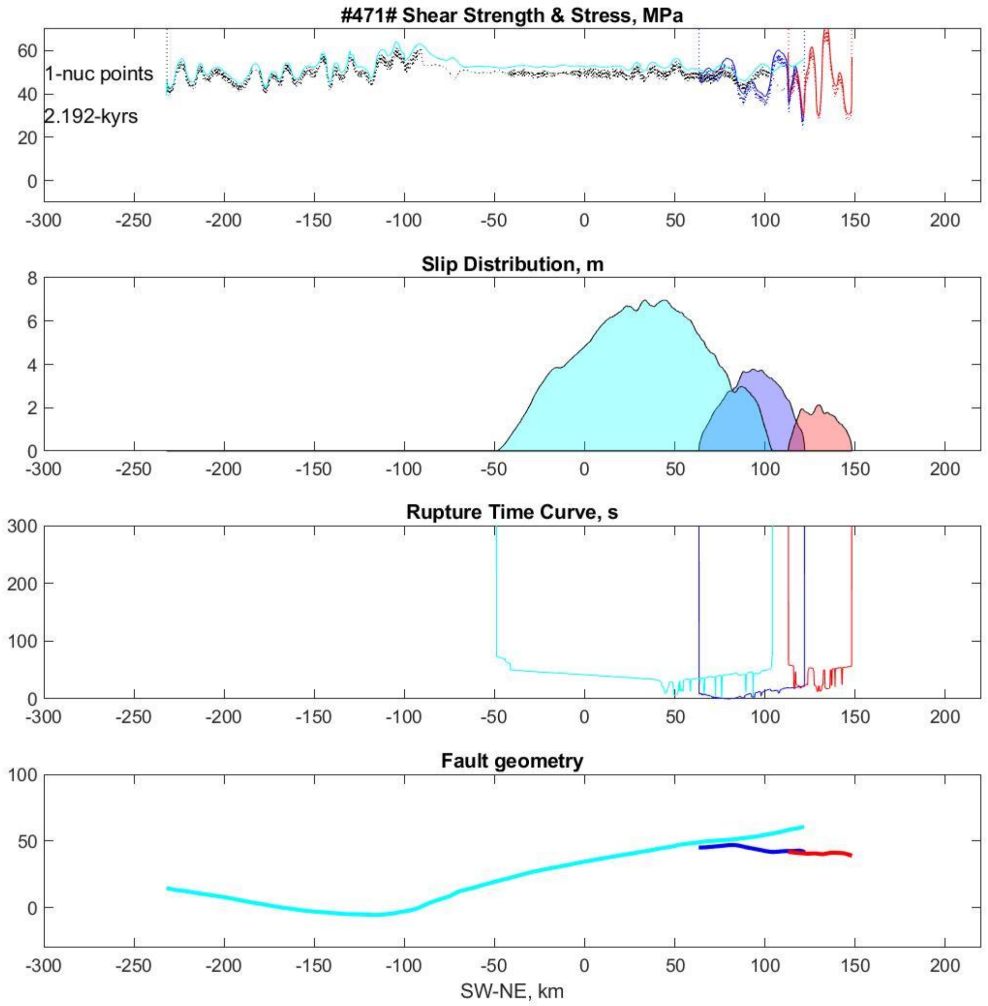

Pingding Shan earthquake gate on Altyn Tagh fault: Explaining complexity in recurrence intervals

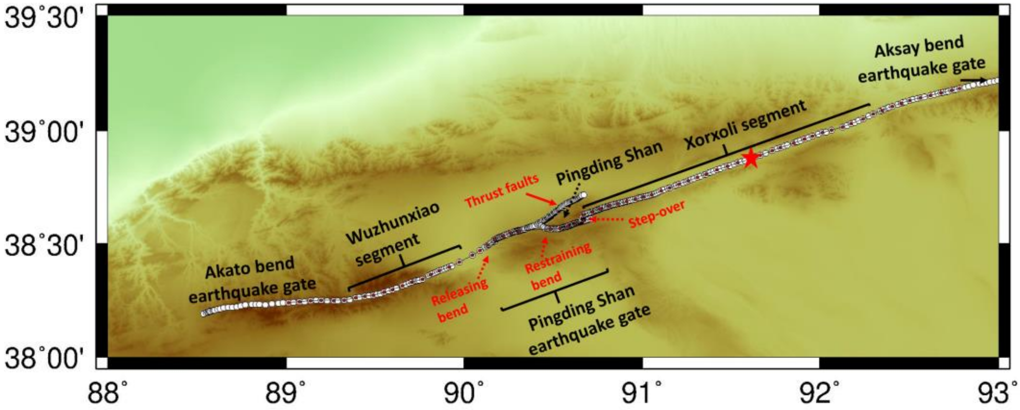

- Complexity from paleoseismological record.
- The Copper Mine site.
- 9 earthquakes over 6000 years with a COV of 0.66 (*Yuan et al.*, 2018).
- Mean and std of recurrence intervals.
- COV, coefficient of variation, = Std/Mean (*Scharer et al.*, 2014; *Williams et al.*, 2019)
- ~0: periodic recurrence
- ~1: random
- >1: clustered

	Simulated Model A	**Observation**
Mean of recurrence interval	535 years	624 years
Std of recurrence interval	362 years	412 years
COV (Std/Mean)	0.675	0.660
Numbers of events	62	9